Decay of a narrow
and high spin ^{24}Mg + ^{24}Mg resonance

M.-D. Salsac [a,*], F. Haas [a], S. Courtin [a], A. Algora [b], C. Beck [a],
S. Beghini [c], B.R. Behera [d], R. Chapman [e], L. Corradi [d], Z. Dombradi [b],
E. Farnea [c], E. Fioretto [d], A. Gadea [d], D.G. Jenkins [f], A. Latina [d],
D. Lebhertz [a], S. Lenzi [c], X. Liang [e], N. Marginean [d], G. Montagnoli [c],
D. Napoli [d], P. Papka [a], I. Pokrovski [d], G. Pollarolo [g], M. Rousseau [a],
E. Sahin [d], A. Sanchez i Zafra [a], F. Scarlassara [c], D. Sohler [b],
A.M. Stefanini [d], S. Szilner [h], M. Trotta [i], C. Ur [c], F. Della Vedova [d],
Z.M. Wang [d], K.T. Wiedemann [d]

[a] *IPHC, Université Louis Pasteur, CNRS-IN2P3, Strasbourg, France*
[b] *INR, Debrecen, Hungary*
[c] *Università di Padova and INFN, Padova, Italy*
[d] *INFN Laboratori Nazionali di Legnaro, Legnaro, Italy*
[e] *University of the West of Scotland, Paisley, UK*
[f] *University of York, York, UK*
[g] *Università di Torino and INFN, Torino, Italy*
[h] *RBI, Zagreb, Croatia*
[i] *Università di Napoli and INFN, Napoli, Italy*

Abstract

The ^{24}Mg + ^{24}Mg reaction has been studied at the Legnaro Tandem at a CM bombarding energy of 45.7 MeV where a narrow and high spin resonance has been reported previously. The decay of the resonance into the inelastic and fusion–evaporation channels has been investigated. The ON and OFF resonance decay yields have been measured using, for the inelastic channels, the fragment spectrometer PRISMA and the γ array CLARA, and, for the fusion–evaporation channels, the Si array EUCLIDES and the γ array GASP. Strong resonant effects have been observed in the inelastic channels involving the 2_1^+ and 4_1^+ states of

* Corresponding author.
  E-mail address: marie-delphine.salsac@ires.in2p3.fr (M.-D. Salsac).

the ^{24}Mg ground state band. Weaker effects are also seen in certain fusion–evaporation channels. The properties of the studied resonance are in agreement with molecular model predictions. It is also proposed that the narrow and high spin ^{24}Mg + ^{24}Mg resonance corresponds to the formation of a fast rotating and highly prolate deformed ^{48}Cr after a Jacobi shape transition and just before fission.

1. Introduction

Resonant phenomena are well established in light heavy-ion collisions. They have been mainly observed in the excitation functions for elastic and inelastic channels of reactions with composite systems between ^{24}Mg(^{12}C + ^{12}C) and ^{56}Ni(^{28}Si + ^{28}Si). It has been shown that the observation of resonances in certain systems is well understood in terms of the number of open reaction channels [1–3]. This observation is favoured for systems with a small number of open channels, but the connection between resonances and molecular states in the composite system is still under question. Such a connection can only be firmly established through measurements of their spins and parities, fragment and gamma decay widths.

To better determine this link, the best cases to study are the systems for which the resonance width is narrow (around 100 or 200 keV), which implies that the lifetime of the composite system is long and this would thus justify the assimilation of the formed dinucleus to a nuclear molecule. These conditions are fulfilled for the reaction ^{24}Mg + ^{24}Mg, where narrow resonance phenomena occur at high spin and high excitation energy, which could correspond to molecular states in ^{48}Cr.

Our present study is focused on the decay of a narrow ^{24}Mg + ^{24}Mg resonance at a CM energy of 45.7 MeV, whose properties (spin and width) are well known: $J^\pi = 36^+$ and $\Gamma = 170$ keV [4,5]. Moreover the resonance is located at twice the Coulomb barrier and the corresponding excitation energy of the ^{48}Cr is around 60 MeV. The goal of our two experiments was to measure for this reaction the ON and OFF resonance decay yields into the various inelastic and fusion–evaporation channels.

Before presenting our experimental results, some general considerations about the possible analogy between this ^{24}Mg + ^{24}Mg narrow and high spin resonance and a very deformed ^{48}Cr dinucleus will be given. A resonance width of 170 keV implies a lifetime of 4×10^{-21} s, this is more than 10 times longer than a typical nuclear lifetime and corresponds to a rotation of about 2 turns of the composite system, which gives credit to the possible formation of a ^{48}Cr dinucleus in the resonance process. Therefore, we suggest that there is a possibility of a strong overlap between the entrance channel ^{24}Mg + ^{24}Mg resonance and the very deformed prolate ^{48}Cr nucleus at spin $J^\pi = 36^+$ and excitation energy of 60 MeV.

As the aim of our experiments is to establish the link between the resonance and the molecular state, the first experiment has been focused on the decay of the resonance into the inelastic channels, channels which are ten times stronger than the α transfer channel [6]. This selectivity is in agreement with the molecular model proposed by Uegaki and Abe [7,8] to describe the ^{24}Mg + ^{24}Mg high spin resonances. In order to see the effect of the resonance, the reaction ^{24}Mg + ^{24}Mg has been measured ON and OFF resonance at the Legnaro XTU Tandem using the

PRISMA spectrometer for the detection of the ^{24}Mg fragments and the CLARA array for the γ emitted in coincidence.

In previous experiments [6,9], it has been shown that resonant flux is missing in the ^{24}Mg + ^{24}Mg inelastic channels, therefore the fusion–evaporation channels have been investigated in a second experiment performed also at the Legnaro Tandem with the γ-array GASP coupled to the EUCLIDES detector for the detection of the evaporated light charged particles in coincidence with the γ from the residues.

In the forthcoming sections, the experimental methods used, the results obtained and a discussion will be given for these two experiments.

2. Experimental methods and results

2.1. The ^{24}Mg + ^{24}Mg experiments

The ^{24}Mg + ^{24}Mg reaction has been carried out at the Legnaro XTU Tandem in order to study the $J^{\pi} = 36^{+}$ resonance. As our two experiments on the de-excitation into the inelastic and fusion–evaporation channels are complementary, they have been done in the same conditions. Therefore both measurements were performed ON and OFF resonance with a beam and a target of ^{24}Mg at a bombarding energy of $E_{CM} = 45.7$ MeV. Concerning the first experiment, the setup allowed to register coincidences between fragments and γ rays using the PRISMA spectrometer [10] and the CLARA array [11]. The goal of this experiment was to determine which states in the fragments of the inelastic channels carry away resonance decay strength. As mentioned earlier, missing resonant flux has been searched for in the fusion–evaporation channels. This was the goal of the second experiment done with GASP [12,13] and EUCLIDES [14] for coincidences between γ rays and light charged particles.

The ^{24}Mg beam was produced and accelerated by the Tandem, a negative MgH^{-} ion was extracted from the ion source and then stripped at the terminal accelerator giving a ^{24}Mg in a 7^{+} charge state. The intensity of this ^{24}Mg beam was between 5 and 7 pnA. The laboratory beam energy was 91.72 MeV for the ON resonance measurement and 92.62 MeV for the OFF resonance measurement. The absolute precision of the 90° analysing magnet is 1.2×10^{-3}, consequently for an energy of 91.72 MeV, the precision is 110 keV. This precision is adequate for the present measurement, as the width of the resonance is 170 keV in the center of mass. Special care has been taken in the adjustment of the 90° analysing magnet in order to avoid hysteresis effects and its slits have been closed as much as possible to improve the energy precision.

The target consisted of a thin ^{24}Mg film with a thickness of 40 μg/cm^2 deposited on a 15 μg/cm^2 ^{12}C backing. The thickness of the target was the result of a compromise which took into account the narrow resonance width and the counting rate of a fragment-γ coincidence experiment. Even if the target was conserved under vacuum, a ^{16}O contamination during its installation in the scattering chamber can not be avoided. Concerning the first experiment, because of the ^{16}O and ^{12}C (target backing) contaminations and as only one fragment has been detected in PRISMA, we had to check carefully the binary character of the events collected.

A crucial point of the analysis was the normalization of the ON and OFF resonant results. For the PRISMA/CLARA experiment, we have used a Si monitor detector placed in the reaction chamber, which allows to measure the total number of produced fragments. For the GASP/EUCLIDES experiment, a Faraday cup was used to record the beam integrated charge.

2.2. De-excitation of the resonance into the inelastic channels: The PRISMA and CLARA experiment

From previous experiments [4], it is known that in the ^{24}Mg $+ ^{24}$Mg reaction, resonant effects are observed in both the elastic and inelastic $(0_1^+, 0_1^+)$, $(2_1^+, 0_1^+)$ and $(2_1^+, 2_1^+)$ channels involving the first two members of the ^{24}Mg ground state (g.s.) band. In these experiments, where only fragments were detected and consequently limited energy resolution achieved, the contribution to the resonant process of higher lying states could not be determined. It was the goal of the present experiment to get information concerning the ON versus OFF feeding of the 4_1^+ and 6_1^+ members of the g.s. band and also of members of the $K^\pi = 2^+$ band. In order to have a better resolution, not only the fragments were detected but also the coincident γ rays. The ^{24}Mg fragments produced in the reaction were detected and identified in the PRISMA spectrometer, whereas the gamma emitted in coincidence were recorded in CLARA. This setup allowed us to study the resonance decay into the inelastic channels.

2.2.1. Experimental setup

The goal of PRISMA is the identification of the reaction products in their nuclear charges (Z), masses (A) and energies [15]. The main characteristics of PRISMA are a large solid angle of $\sim$80 msr and a large energy acceptance of $\pm$20%. A position-sensitive micro-channel plate (MCP) detector [16], placed at the entrance of the spectrometer, provides the position signals and also a start signal for the time-of-flight (ToF) measurements. After the magnetic elements, ions enter the focal plane which is made of a parallel plate of multiwire type (MWPPAC) detector [17] providing timing and position signals, and an array of multi-parametric ionization chambers (IC), providing the nuclear charge (through ΔE) and the total energy (E). In the present measurement the PRISMA spectrometer was placed at 43° (covering the angular range of 43° $\pm$ 6°), close to $\Theta_{c.m.} = 90°$ where resonances in the studied reaction have already been observed. Our main interest lays in the excitation energy range between 4.1 and 6.1 MeV, therefore the dipole fields have been adjusted to have $E^* = 5.1$ MeV at the center of the focal plane. In this excitation energy region, there could be a competition between the g.s. band contribution $(0_1^+, 2_1^+, 4_1^+)$ and the contribution due to the feeding of the 2_2^+, 3_1^+ and 4_2^+ members of the $K^\pi = 2^+$ band. This band has been observed to be selectively populated in the resonant radiative capture ^{12}C$(^{12}$C, $\gamma)^{24}$Mg reaction [18], hence it could also play a role in the case of the studied reaction.

The identification of the nuclear charge is obtained through the measurement of the ΔE energy loss in the IC. To take properly into account a broad range of kinetic energies and directions of the ions that reaches the IC, the path (Range) of the ions in the entire spectrometer was determined. An example of such Range versus total energy matrix is displayed in Fig. 1, illustrating the clear Z selection. In this spectrum the fragments come from the reactions ^{24}Mg on ^{24}Mg and ^{12}C (backing). It is seen that the α-like ^{12}C, ^{16}O, ^{20}Ne, ^{24}Mg and ^{28}Si nuclei are preferentially populated compared to the odd Z nuclei, this is due to Q-value effects.

The determination of the mass of the fragments is obtained via an event-by-event reconstruction of the trajectory inside the magnetic elements. From such reconstruction, using the measured positions, the ToF, and the known magnetic fields, the trajectories are uniquely determined. As it is well known, a magnetic spectrometer provides the ratio of the momentum over the atomic charge state, which are related to the bending radius and to the total path length through the magnetic elements, both determined in the trajectory reconstruction. To finally obtain the masses, the atomic charge state selection has to be performed. In Fig. 2, the atomic charge state q distribution is plotted as a function of the longitudinal position X on the focal plane (proportional to
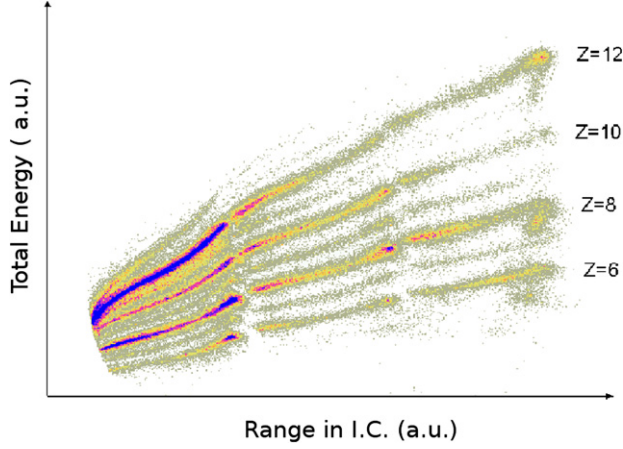
Fig. 1. Z distributions obtained in the PRISMA ionization chambers (IC) of the ^{24}Mg induced reactions on a ^{24}Mg target with ^{12}C backing.
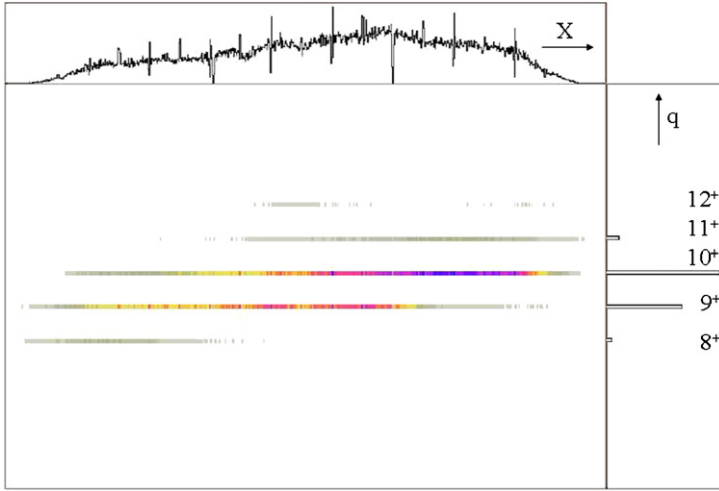

Fig. 2. The ^{24}Mg fragments: position X on the focal plane versus charge state distribution q.

the magnetic rigidity). The large acceptance of the spectrometer is clearly reflected in the fact that different atomic charge states cover different part of the focal plane. In the case of ^{24}Mg fragments, the 9^+ and 10^+ charge states are predominant. For each Z, the fragment data have been analysed ionic charge state by ionic charge state to check whether the parameters of the events collected (angle, velocity) fulfilled the kinematics of true binary events in an experiment which was in fact a 'one arm' experiment.

It has been checked that the angles and the energies of the ^{12}C, ^{16}O, ^{20}Ne, ^{24}Mg and ^{28}Si detected fragments are in agreement with their corresponding values calculated from the kinematics of the ^{24}Mg on ^{24}Mg (target), ^{12}C (backing) and ^{16}O (contaminant). For the ^{24}Mg on ^{12}C and ^{16}O, the ^{24}Mg fragments can not reach the focal plane due to limiting angle (30° in the case of ^{24}Mg on ^{12}C) and energy considerations.
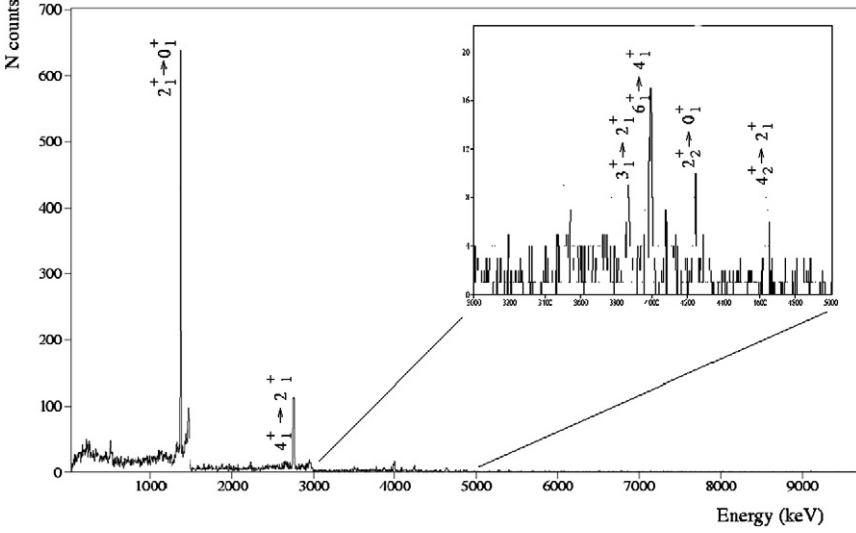
Fig. 3. Gamma spectrum of the ^{24}Mg + ^{24}Mg reaction recorded in coincidence with ^{24}Mg fragments.

The prompt γ rays emitted by the fragments have been detected in coincidence using CLARA, which is composed of 24 clovers, each of them consisting in 4 Ge HP crystals. Each detector is surrounded by a BGO anti-Compton shield, allowing a significant improvement of the photopeak-to-total ratio.

The γ spectrum in coincidence with the selected ^{24}Mg fragments is shown in Fig. 3. An accurate determination of the fragment velocity vector in PRISMA allows a rather precise Doppler correction of the corresponding γ-ray energy spectrum. For a fragment velocity of $\beta = 6\%$, a 0.6% resolution has been obtained for the $2_1^+ \rightarrow 0_1^+$ ^{24}Mg transition with $E_\gamma = 1369$ keV.

In the γ spectrum in Fig. 3, the two predominant lines correspond to the ^{24}Mg transitions $2_1^+ \rightarrow 0_1^+$ with $E_\gamma = 1369$ keV and $4_1^+ \rightarrow 2_1^+$ with $E_\gamma = 2753$ keV, where the 0_1^+, 2_1^+ and 4_1^+ are the first members of the ^{24}Mg $K^\pi = 0^+$ g.s. band. At higher energies, weaker lines are observed (see the inset of Fig. 3), they correspond to transitions with $E_\gamma = 3991$ keV ($6_1^+ \rightarrow 4_1^+$), 3867 keV ($3_1^+ \rightarrow 2_1^+$), 4238 keV ($2_2^+ \rightarrow 0_1^+$) and 4642 keV ($4_2^+ \rightarrow 2_1^+$). The 6_1^+ level belongs to the g.s. band and the 2_2^+, 3_1^+ and 4_2^+ to the ^{24}Mg $K^\pi = 2^+$ band. Looking at the γ spectrum in Fig. 3 and at the two strongest lines, broad components lying beneath the narrow lines can be observed. They correspond to incorrectly Doppler corrected γ rays emitted by the non-detected ^{24}Mg of the ^{24}Mg + ^{24}Mg binary exit channel. From this γ spectrum, even if the γ-ray efficiency of CLARA varies as $\sim 1/E_\gamma$ and its absolute efficiency is 3.7% at 1 MeV and 0.9% at 4 MeV, it is already clear that the inelastic channels are dominated by the feeding of the 2_1^+ and 4_1^+ states in ^{24}Mg. This important fact will be explicitly discussed in the following section.

2.2.2. Experimental results

The Q-value spectrum of the ^{24}Mg + ^{24}Mg inelastic channels is represented in Fig. 4. From left to right, four different peaks can be observed on the spectrum. The first one corresponds to the binary channel $2_1^+ - 0_1^+$, the second one mainly to the excitation $2_1^+ - 2_1^+$ and the third and fourth one principally to the excitation $4_1^+ - 2_1^+$ and $4_1^+ - 4_1^+$. The general shape and covered
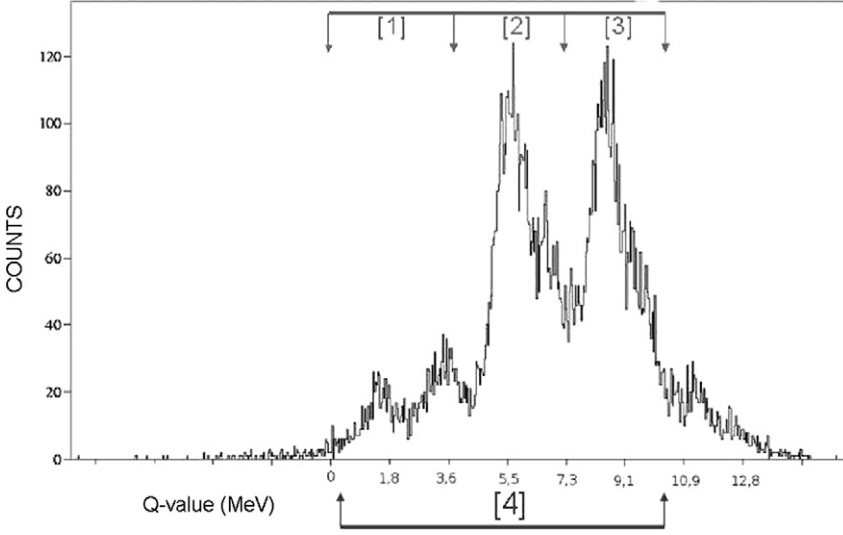
Fig. 4. Q-value spectrum of the ^{24}Mg + ^{24}Mg inelastic channels with indication of the different gates considered (see text).

Q-value region of the spectrum are due to the setting of the PRISMA dipole which favoured the excitation region between 4 and 6 MeV.

Four different gates have been defined on the Q-value spectrum shown in Fig. 4. The first gate ranges from 0.3 to 4.1 MeV, which corresponds to the excitations $2_1^+ - 0_1^+$ and $2_1^+ - 2_1^+$. The second gate corresponds to the excitation energy from 4.1 to 6.9 MeV, which is our region of main interest (dominant contribution comes from excitation $4_1^+ - 2_1^+$). In the third gate, there is a dominant contribution from $4_1^+ - 4_1^+$, which corresponds to an excitation energy from 6.9 to 10 MeV. Finally, gate 4 includes the 3 latter gates.

In order to determine which states in the inelastic channels carry away the resonant flux, the yields of the corresponding γ-ray transitions have been measured both ON and OFF resonance energies. In Fig. 5 is represented the ratio R of these yields for different transitions and selected Q-value gates, if R equals 1 there is no resonant effect. The first gate on Q corresponds to an inelastic excitation energy between 0.3 and 4.1 MeV and thus to the ^{24}Mg channels $(2_1^+, 0_1^+)$, $(2_1^+, 2_1^+)$ and $(4_1^+, 0_1^+)$. For both transitions $2_1^+ \rightarrow 0_1^+$ and $4_1^+ \rightarrow 2_1^+$, R equals approximately 2 and thus both 2_1^+ and 4_1^+ states are resonant states, the strongest contribution in this gate comes from the $(2_1^+, 2_1^+)$ channel. The second gate on Q-value corresponds to an excitation energy between 4.1 and 6.9 MeV. For this gate, a resonant effect is seen again in the yields of the $2_1^+ \rightarrow 0_1^+$ and $4_1^+ \rightarrow 2_1^+$ transitions. In this gate, the main contribution comes from the $(4_1^+, 2_1^+)$ channel. The ratio R for $2_1^+ \rightarrow 0_1^+$ is smaller than for $4_1^+ \rightarrow 2_1^+$, this can probably be explained by a weak feeding of 2_1^+ by states of the $K^\pi = 2^+$ band, which will be shown later to be non-resonant. The third gate corresponds to an excitation energy between 6.9 and 10 MeV. As before, a resonant effect is seen in the yields of $2_1^+ \rightarrow 0_1^+$ and $4_1^+ \rightarrow 2_1^+$, in this gate the main contribution comes from the $(4_1^+, 4_1^+)$ channel. Finally the fourth gate corresponds to the total excitation energy from 0.3 to 10 MeV. The $2_1^+ \rightarrow 0_1^+$ and $4_1^+ \rightarrow 2_1^+$ show strong resonant effects, the yields of the other transitions (see the inset of Fig. 3) are weak and non-resonant ($R \sim 1$).
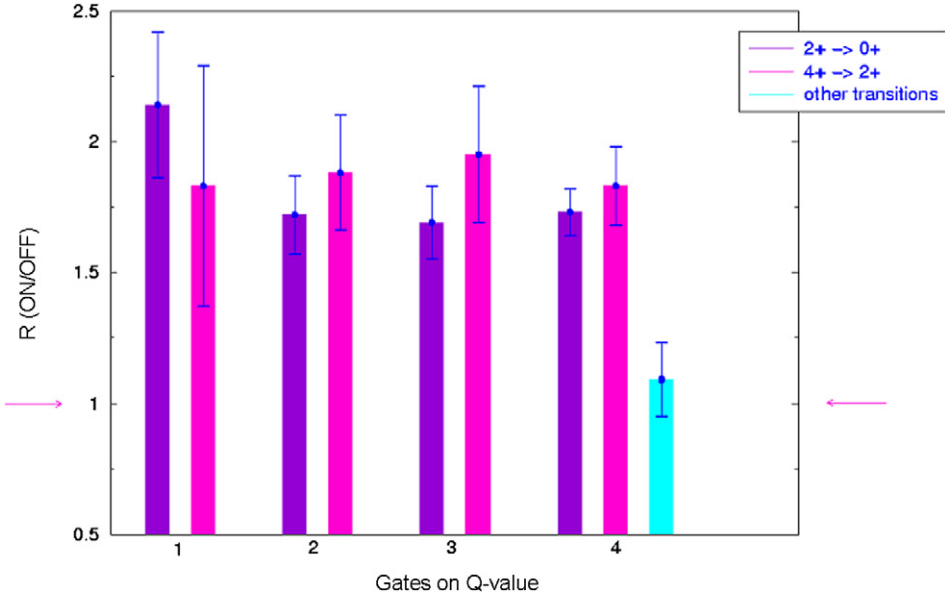
Fig. 5. ON and OFF yield ratios R for different ^{24}Mg transitions and Q-value gates.
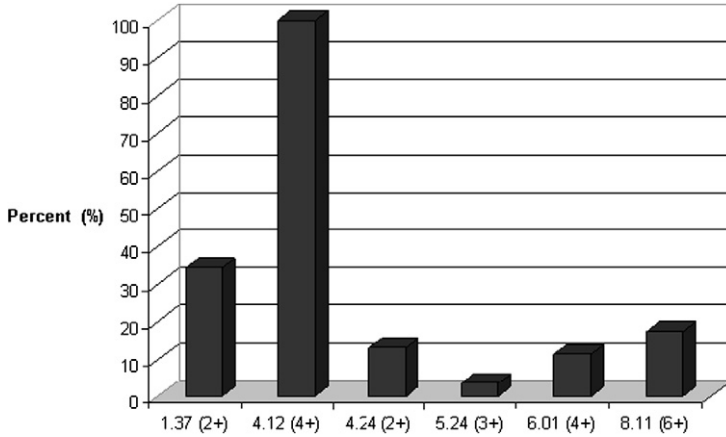

Fig. 6. ON resonance direct feeding of the ^{24}Mg states in the ^{24}Mg + ^{24}Mg inelastic channel.

The ON and OFF resonance ratio R allows to determine the resonant states in the ^{24}Mg + ^{24}Mg reaction. In the g.s. band of ^{24}Mg, the 2_1^+ and 4_1^+ are the resonant states. The 6_1^+ and the different states in the $K^\pi = 2^+$ band are shown to be non-resonant. As shown in Fig. 5, a R ratio of ∼2 has been deduced for the resonant states. This is in very good agreement with the ON/OFF resonance yield observed in previous excitation function measurements [4] in the elastic and low lying inelastic channels.

For the ON resonance measurement, the direct feeding yields of the different ^{24}Mg states have been extracted and are represented in Fig. 6. All the feeding contributions from higher states have been subtracted and the CLARA efficiency has been taken into account. It is obvious that for the

^{24}Mg excitation energy region investigated in our experiment, the 2_1^+ and moreover the 4_1^+ play an essential role in the decay of the ^{24}Mg + ^{24}Mg resonance.

To conclude, for the $J^\pi = 36^+$ resonance at $E_{CM} = 45.7$ MeV, the resonant decay flux in the inelastic channels for an excitation region between 0 and 10 MeV goes to the 2_1^+ and 4_1^+ states of the g.s. band of ^{24}Mg.

2.3. De-excitation of the resonance into the fusion–evaporation channels: The GASP and EUCLIDES experiment

In the previous sections, we have presented the results on the de-excitation of the $J^\pi = 36^+$ resonance in the inelastic channels. For the ^{24}Mg + ^{24}Mg resonance at $E_{CM} = 45.7$ MeV, the resonant flux in the inelastic channels represents only 30% of the total resonant flux [5,9]. Therefore the question of where the missing flux goes is still an open question. At the considered bombarding energy of the ^{24}Mg + ^{24}Mg reaction, the fusion–evaporation cross section is equivalent to 80% of the reaction cross section [19,20]. This is the reason why a second experiment has been performed in order to search for missing flux in the strong fusion–evaporation channels. More precisely, we are looking for selective feeding of fusion–evaporation nuclei or of specific states of those nuclei by the ^{24}Mg + ^{24}Mg resonance.

At our bombarding energy, the fusion cross section equals 1060 mb [19,20]. The sharp cut-off model predicts an angular momentum of 28 for this energy, which is 8 units lower than the $J = 36$ resonant spin. As far as this schematic model is concerned, the L distribution in the compound nucleus would not allow a significant contribution of the resonant $L = 36$ momentum to the fusion process. However, the inclusion of the coupling to the excited states of both projectile and target could extend the L distribution in the compound nucleus to much higher values, even up to $L = 36$ [21]. In the extreme case of complete fusion for the resonant partial wave $L = 36$, the corresponding partial fusion cross section is 175 mb, which would represent ∼16% of the total measured fusion cross section. It can thus be expected that an eventual effect in the fusion channels would be smaller than this but still represent a significant cross section. In these conditions, some of the resonant flux could be absorbed in the fusion–evaporation channels.

On top of that, a spin of 36 is very close to an angular momentum of 38–40 for which it is predicted that the ^{48}Cr fission barrier vanishes [22], it is also worth mentioning that at the resonance energy, the grazing angular momentum equals 32, which is 4 units lower than the resonant spin. Due to all these considerations, the resonant spin of 36 corresponds to a very unique situation for which the decay has to be exotic.

To look for the fusion–evaporation channels, the GASP array has been used to record the γ rays from the residues in coincidence with EUCLIDES for the light charged particles emitted in the fusion–evaporation process.

2.3.1. Experimental setup

EUCLIDES (EUropean Charged Light Ions DEtector Sphere) is a 4π detector, composed of 40 Si detectors $\Delta E - E$ (130 μm–1 mm) used for the detection of the light charged particles emitted in the fusion–evaporation process. With the used target and absorbers placed in front of the detector, the efficiency for the proton (p) detection is 60%, whereas the efficiency for the α is 35%.

In coincidence with p and α, the γ rays from the residues are detected in GASP (GAmma ray SPectrometer), a 4π detector composed of 40 HP Ge detectors. As the GASP array was used in its configuration close to the target, the photopeak efficiency for the 1.33 MeV γ-ray of
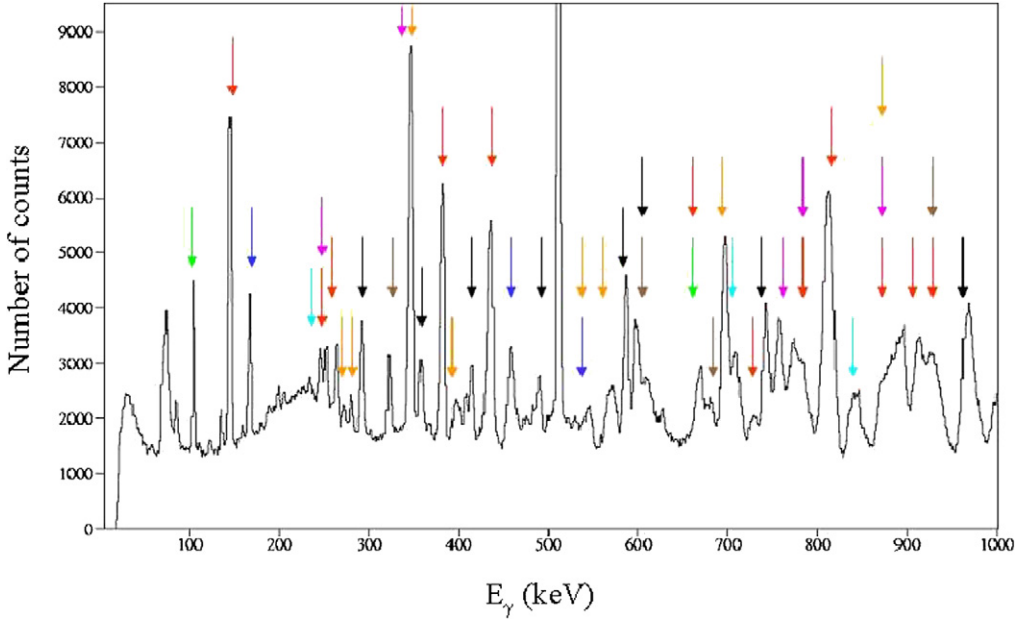
Fig. 7. The ^{24}Mg + ^{24}Mg reaction and the $\gamma-\gamma$ spectrum for an angle of 90° and $E_\gamma < 1$ MeV. The different arrows are discussed in the text.

Table 1
Nuclei from the ^{24}Mg + ^{24}Mg reaction with the fusion–evaporation channels and the γ observed (see text for more details)

Nuclei	Channels	E_γ (keV)
^{45}Ti	$2pn$	293, 359, 415, 483, 586, 592, 655, 743, 897, 980, 1138, 1189, 1248, 1468, 1547, 1818
^{44}Sc	$3pn$	167, 235, 271, 281, 350, 357, 396, 546, 566, 697, 895, 1703
^{42}Ca	$\alpha 2p$	145, 253, 264, 382, 437, 665, 728, 772, 810, 815, 874, 910, 918, 929, 1228, 1347, 1525, 1644, 1733, 1965, 2301, 2555, 2955, 3220
^{41}K	$\alpha 3p$	247, 708, 850, 1123, 1500, 1513, 1677
^{41}Ca	$\alpha 2pn$	168, 460, 545, 1389, 1607, 3201, 3370
^{39}K	$2\alpha p$	252, 347, 757, 783, 887, 1129, 1301, 1342, 1410, 1774, 1881, 2490, 2814, 3197, 3597
^{38}Ar	$2\alpha 2p$	106, 670, 1643, 1822, 2167
^{37}Ar	$2\alpha 2pn$	323, 598, 680, 937, 1264, 1506

^{60}Co is 5.8%. The 40 detectors of GASP are clustered in 7 rings which correspond to different angles going from 35° up to 145°. Of special interest for the analysis was ring 4 located at 90° and showing consequently only a Doppler broadening and no Doppler shift. Due to the target composed of ^{24}Mg on a ^{12}C backing, the reactions ^{24}Mg on ^{24}Mg and ^{24}Mg on ^{12}C form two compound nuclei ^{48}Cr and ^{36}Ar, for which the velocity β was 4.5% and 6%, respectively.

The goal of this experiment was to look for the selective feeding of the different fusion–evaporation channels by the resonant reaction, the produced residues have thus to be identified. For this purpose, both GASP and EUCLIDES have been used, but the best selectivity and statistics were obtained in the $\gamma-\gamma$ spectra which enable to identify properly the different fusion–evaporation channels. Fig. 7 shows the $\gamma-\gamma$ spectrum at an angle of 90° for $E_\gamma < 1$ MeV, in fact
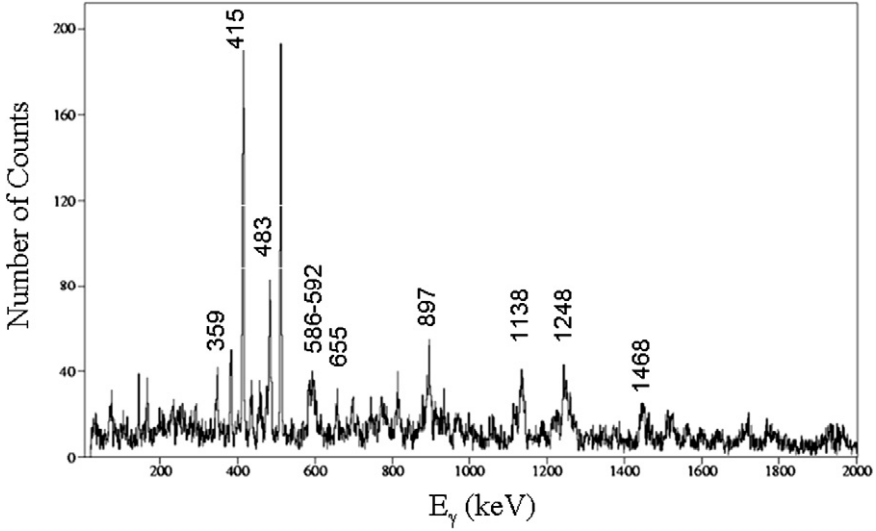
Fig. 8. The γ-ray spectrum of the $2pn$ ^{45}Ti fusion channel with a gate on the 293 keV γ peak.

all the residues produced by the ^{24}Mg + ^{24}Mg reaction have γ rays with energies below 1 MeV. In order to identify the lines, 'coloured' arrows have been placed on each line of Fig. 7. Table 1 indicates the connection between the 'colours' and the residues and gives also the γ observed in each residue and the corresponding fusion–evaporation channels.

Eight nuclei are observed in the ^{24}Mg + ^{24}Mg reaction: ^{45}Ti, ^{44}Sc, ^{42}Ca, ^{41}K, ^{41}Ca, ^{39}K, ^{38}Ar and ^{37}Ar and all the details concerning the transitions observed are summarized in Table 1. In Fig. 7, the γ lines lower than 100 keV correspond to X rays from lead shieldings, the first line of the ^{24}Mg + ^{24}Mg reaction located at 106 keV (green arrow) belongs to the $2\alpha 2p$ ^{38}Ar channel. Four other γ rays can be observed in this nucleus from 670 keV to 2167 keV. The second line at 145 keV is one of the ^{42}Ca lines ($\alpha 2p$ channel—red arrow). The ^{42}Ca nucleus is very strongly fed in the experiment and several lines have been seen. It is the same for the ^{39}K nucleus ($2\alpha p$ channel—pink arrow). Two nuclei with $A = 41$ are observed in this spectrum, i.e. ^{41}Ca ($\alpha 2pn$ channel—dark blue arrow) and ^{41}K ($\alpha 3p$ channel—light blue arrow). Finally, several lines from the ^{44}Sc ($3pn$ channel—orange arrow), ^{45}Ti ($2pn$ channel—black arrow) and ^{37}Ar ($2\alpha 2pn$ channel—brown arrow) are also seen in this spectrum.

All the marked lines have been identified to be γ transitions from nuclei produced in the ^{24}Mg + ^{24}Mg reaction. In the next section, γ transitions of the different residues will be analysed in order to find selective feeding of their states.

2.3.2. Experimental results

In order to get an idea of which type of states are populated in the residues, we will first consider the case of ^{45}Ti, the residue closest to the ^{48}Cr compound nucleus, and which has been produced in the ^{24}Mg + ^{24}Mg reaction via the evaporation of 2 protons and 1 neutron. To get an accurate view of the different states fed by the reaction, gates have been placed on γ belonging to ^{45}Ti in the $\gamma-\gamma$ spectrum.

Fig. 8 is obtained by gating on the 293 keV, $3/2^+ \rightarrow 3/2^-$ transition (see Fig. 9), the peaks observed on the figure are in coincidence with this transition. A few of them are quite strong
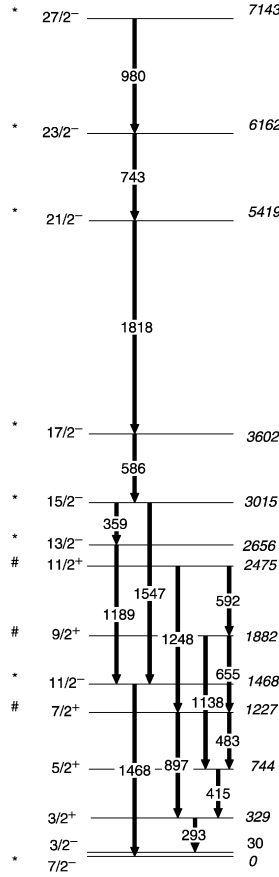
Fig. 9. Level scheme observed for the $2pn$ ^{45}Ti fusion channel. The yrast levels are indicated by * and the yrare states by ♯.

such as the 415 keV ($5/2^+ \rightarrow 3/2^+$), 483 keV ($7/2^+ \rightarrow 5/2^+$), 897 keV ($7/2^+ \rightarrow 3/2^+$) and 1248 keV ($11/2^+ \rightarrow 7/2^+$), as they are situated just above the 'gating' transition $3/2^+ \rightarrow 3/2^-$.

The spectrum represented in Fig. 10 is the result of the gate set on the 586 keV line corresponding to the transition $17/2^- \rightarrow 15/2^-$. Contrary to the 293 keV line, this transition is between two yrast states (see Fig. 9), which explains why the γ observed in coincidence are very intense. All these transitions are between yrast states such as the lines at 359 keV ($15/2^- \rightarrow 13/2^-$), 743 keV ($23/2^- \rightarrow 21/2^-$), 980 keV ($27/2^- \rightarrow 23/2^-$), 1468 keV ($11/2^- \rightarrow 7/2^-$), 1547 keV ($15/2^- \rightarrow 11/2^-$) and 1818 keV ($21/2^- \rightarrow 17/2^-$).

The ^{45}Ti case shows clearly that the yrast states take most of the flux and are preferentially fed by the reaction. The larger flux observed in the spectrum of Fig. 10 compared to the one in Fig. 8 is not only explained by the fact that the γ rays in Fig. 10 are transitions between yrast states but also because the 586 keV gating peak corresponds to a transition located at high angular momentum between the $17/2^-$ and $15/2^-$ states. As usual for a fusion–evaporation channel, we observe that the high spin states are strongly fed which is due to the fact that the compound nucleus high angular momenta populated through the ^{24}Mg + ^{24}Mg entrance channel are carried away preferentially through the yrast states of the residues.
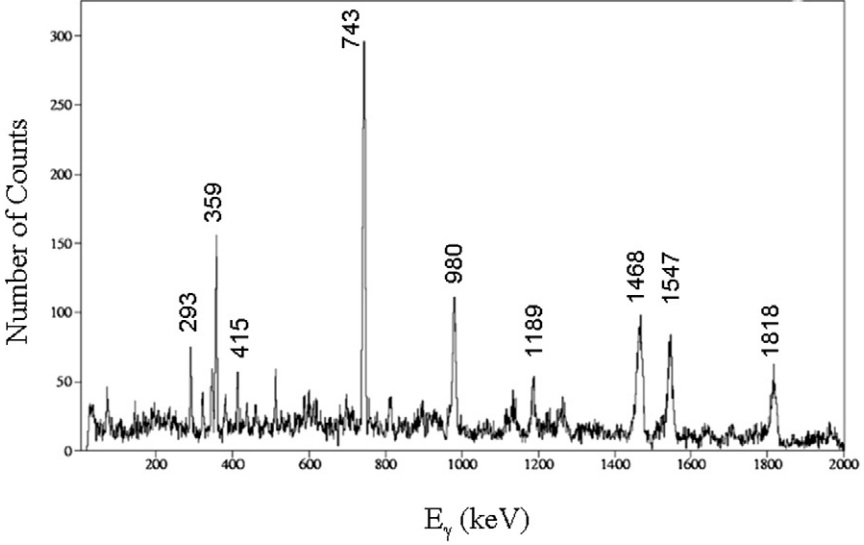
Fig. 10. The γ-ray spectrum of the $2pn$ ^{45}Ti fusion channel with a gate on the 586 keV γ peak.

The eight main nuclei produced by fusion–evaporation of the ^{24}Mg + ^{24}Mg entrance reaction have been studied. As shown in the case of ^{45}Ti, a high selectivity population of the yrast and yrare states has been observed for all the nuclei produced.

For the different transitions observed in the eight residues produced by the ^{24}Mg + ^{24}Mg reaction, we have evaluated the ON/OFF resonance ratio (R). For each gating transition, several ON/OFF intensities ratios have been obtained and the average value of these ratios has been deduced weighed by the errors on each point. The given error on the average has been estimated by the standard deviation of the experimental results and the corresponding result is represented by the two red lines in Fig. 11 in the case of ^{45}Ti and in Fig. 12 in the case of ^{41}Ca.

Fig. 11 gives also R, the ratio ON/OFF resonance for the ^{45}Ti channel. Eight gates have been used for the determination of the ratio of eleven γ rays from an energy of 293 keV to 1818 keV, the average value of R is 1.07 ± 0.02. The different points are lying very close to this mean value except the two higher points at 359 keV and 1818 keV, where the problem is either due to low statistics or to a Doppler broadening effect which both imply large error bars. Another example is shown in Fig. 12, it concerns the $\alpha 2pn$ ^{41}Ca fusion channel for which an average value of $R = 0.92 \pm 0.02$ has been obtained. The cases of ^{45}Ti and ^{41}Ca, with $R > 1$ and < 1 respectively, have been chosen to illustrate the difference observed in the 2 sets of data. The same analysis has been done for the eight observed nuclei and the results are summarized in Table 2. This table gives the strongest channels and nuclei produced via the ^{24}Mg + ^{24}Mg reaction, it gives also for each residue the excitation energy and spin corresponding to the favoured feeding and finally the ON/OFF resonance ratio.

For all studied nuclei, it was found that R did not depend on the γ-ray location in the level scheme which enabled to calculate an average value of the ratio for each case. As seen in Table 2, the selective feeding of the nuclei by the fusion–evaporation process is at high excitation energy and high angular momentum as the ^{48}Cr compound nucleus has an excitation energy of around 60 MeV and spins up to 36 that have to be evacuated into the de-excitation channels. This implies that for these channels the yrast states are preferentially populated.
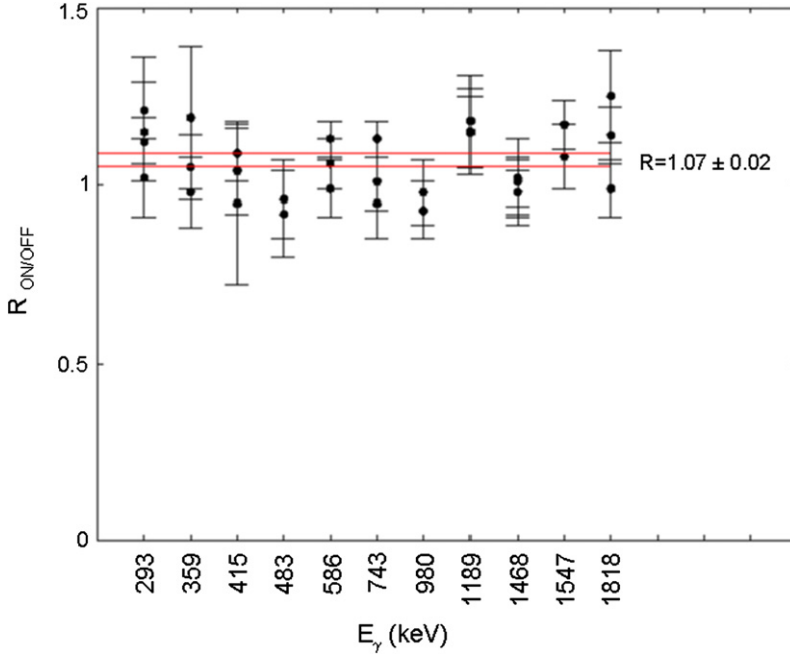
Fig. 11. The ON/OFF resonance ratio of the γ-ray intensities for the indicated transitions in ^{45}Ti. For a given γ-ray energy, the values of R have been obtained using different gating cascade transitions.
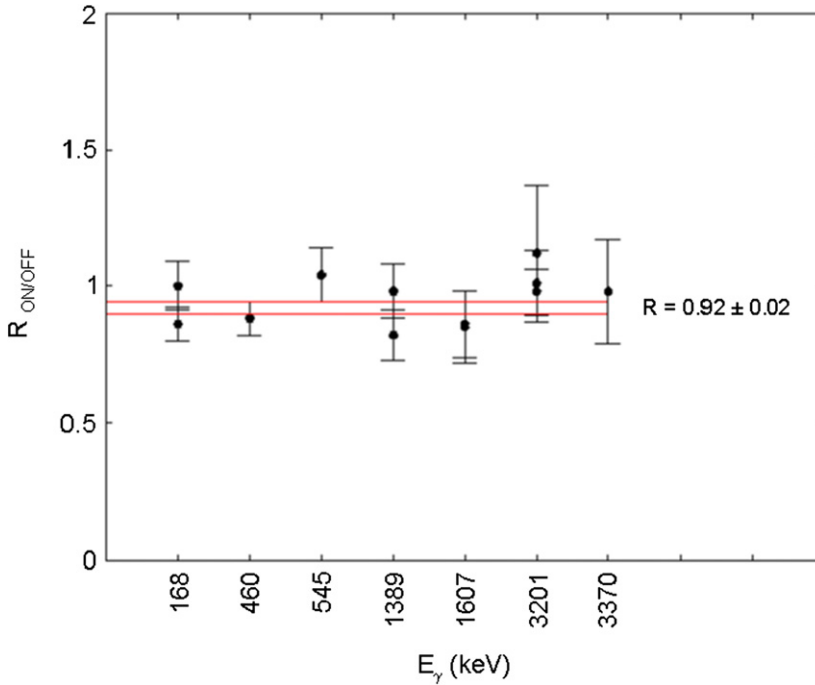

Fig. 12. The ON/OFF resonance ratio of the γ-ray intensities for the indicated transitions in ^{41}Ca.

Table 2
For each residue observed in the ^{24}Mg + ^{24}Mg reaction: channels, excitation energies and spins of favoured feeding, ON/OFF resonance ratios

Nuclei	Channels	E (MeV)	Spins	$R_{ON/OFF}$
^{45}Ti	$2pn$	6.2	12	1.07 ± 0.02
^{44}Sc	$3pn$	3.6	11	0.96 ± 0.02
^{42}Ca	$\alpha 2p$	7.8	11	1.03 ± 0.01
^{41}K	$\alpha 3p$	2.8	7	0.83 ± 0.04
^{41}Ca	$\alpha 2pn$	5.9	9	0.92 ± 0.02
^{39}K	$2\alpha p$	8	10	1.00 ± 0.01
^{38}Ar	$2\alpha 2p$	4.6	5	0.97 ± 0.03
^{37}Ar	$2\alpha 2pn$	6.5	8	0.88 ± 0.03

If a resonant effect exists in the fusion–evaporation channels, the ratio will differ from 1. As can be seen in Table 2, the resonant effect is smaller than the one observed in the inelastic channels presented previously where the ratio equals roughly 2. But due to the experimental cautions taken, we believe that the deviations from 1 are significant and that a resonant effect is present in the fusion–evaporation channels. The ratio is higher or equals 1 for ^{45}Ti, ^{42}Ca and ^{39}K and is lower than 1 for ^{44}Sc, ^{41}K, ^{41}Ca, ^{38}Ar and ^{37}Ar. The maximum difference in R is 0.24 ± 0.05 between ^{45}Ti and ^{41}K. These results will be discussed in the next section.

3. Discussion

In order to study the correlation between resonances and molecular states, the resonant reaction ^{24}Mg + ^{24}Mg has been studied and two experiments have been performed to look at the de-excitation modes of the resonance. The PRISMA/CLARA setup has been used to investigate the inelastic channels and the GASP/EUCLIDES setup to search for resonance flux in the fusion–evaporation channels.

Concerning the results obtained for the inelastic channels, the ^{24}Mg + ^{24}Mg resonance decay flux is essentially observed in the ^{24}Mg 4_1^+ and 2_1^+ states (present measurements) and also in the elastic channel [4,5], i.e. in the first three members of the ^{24}Mg $K^\pi = 0^+$ ground state band. This is in agreement with the molecular model proposed by Uegaki and Abe [7,8] to describe the ^{24}Mg + ^{24}Mg high spin resonances, in which the main collective motions of the system are taken into account and the nucleus–nucleus interaction is described by a folding potential. The equilibrium shape obtained in these calculations is a very deformed prolate pole-to-pole configuration which, as will be shown later, is very similar to the ^{48}Cr shape obtained after a Jacobi transition and before fission. The identification of the $J^\pi = 36^+$ resonance at $E_{CM} = 45.7$ MeV with a ^{48}Cr hyperdeformed molecular state is in agreement with the molecular model predictions what excitation energy, spin and decay are concerned. In this picture, the ground state ^{24}Mg rotational band and especially the 0_1^+, 2_1^+ and 4_1^+ states play the dominant role in the description and in the decay of the resonance as demonstrated in our experiment. We would also like to mention that for the ^{24}Mg + ^{24}Mg system, in the present experimental conditions, the maximum calculated angular momenta transfer to each fragment in a sticking condition is $J = 4$ which is in agreement with our results.

In previous experiments [23,24], the population of the inelastic channels of the ^{24}Mg + ^{24}Mg reaction at an energy of $E_{CM} = 44.4$ MeV was studied with the aim to look at the competition between the resonant and the fusion–fission mechanisms. In this work, it was concluded that the
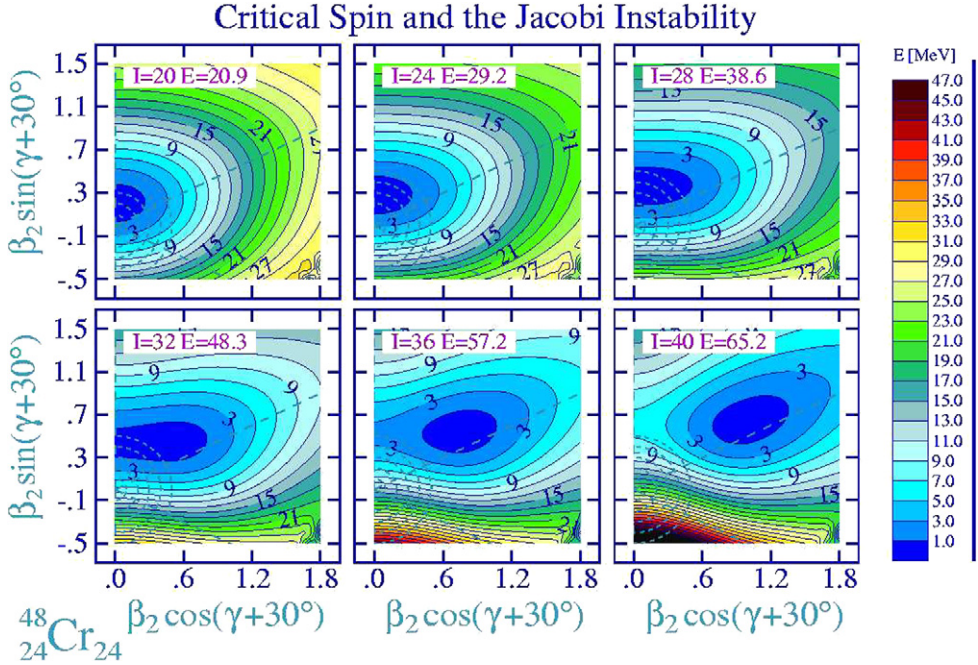
Fig. 13. Total energy calculations in terms of the standard $(\beta - \gamma)$ deformations according to the LSD approach for the nucleus ^{48}Cr at spins I between 20 and 40 [28].

fusion–fission process, which is a statistical phenomenon, is able to explain the inelastic spectra recorded at high excitation energy (above 8 MeV) but not the low excitation energy part, where the resonance effect is dominant. For this lower excitation energy part, the fusion–fission process is responsible for the background seen in the excitation functions of these inelastic channels, whereas the resonances explain the structures observed [23,24]. Unfortunately, these experiments have neither been done ON and OFF resonance nor at the resonance energy of the present work. Nevertheless the conclusions of Refs. [23,24] are in agreement with the present observations, i.e. the resonant flux is only seen in the elastic and inelastic channels involving the first 2_1^+ and 4_1^+ states.

The resonance under study has a very high spin ($J^\pi = 36^+$) and it is known that for the ^{48}Cr nucleus the fission barrier vanishes at spin $\sim$40. For this relatively light nucleus, the rotational frequency close to the fission limit is very large and a Jacobi shape transition can be expected [25]. Calculations of the ^{48}Cr shape evolution were performed using a new version of the liquid drop model that accounts explicitly for the nuclear surface curvature effects. Details concerning the Lublin–Strasbourg–Drop (LSD) approach can be found in Refs. [26] and [27]. The results for ^{48}Cr can be seen in Fig. 13.

For spin $I = 20$ to $I = 24$, the shape of the nucleus is oblate; from $I = 28$ to $I = 32$, the Jacobi transition takes place and the nucleus becomes triaxial; for $I = 36$ (the present resonance spin), the shape is strongly prolate and the excitation energy predicted by this macroscopic model is close to the resonance excitation energy of 60 MeV. Finally, for $I = 40$, the fission barrier gets small and the nucleus is about to fission. This model not only explains why at the resonant spin of 36 the ^{48}Cr is prolate but also gives an equilibrium shape which is very similar to the one obtained through the molecular model by Uegaki and Abe [7,8].

Such similarity of the shape suggests that there is an overlap between the resonance in our ^{24}Mg + ^{24}Mg entrance channel and the prolate ^{48}Cr composite system after the Jacobi shape transition.

In the present work, new experimental results have been obtained concerning the inelastic channels selectively populated in the resonant process. Nevertheless these channels represent only 30% of the resonant flux [5,9], the missing flux is certainly not in the α transfer channel ^{20}Ne + ^{28}Si for which the yield has been shown to be ten times smaller [6]. Therefore it was the goal of the second experiment to look at the fusion–evaporation channels not only to find missing flux but also to search for favoured feeding of deformed nuclei in the evaporation chains. It can be conjectured that a memory of a deformed entrance channel system could persist in the exit channel [29]. As superdeformed bands exist in ^{36}Ar [30], ^{40}Ca [31,32] and perhaps ^{42}Ca [33], it is thus worthwhile to search for a selective feeding of such bands in nuclei which can be formed by the ^{24}Mg + ^{24}Mg fusion–evaporation reaction.

At the used beam energy, the strongest channels produced via the ^{24}Mg + ^{24}Mg reaction are ^{45}Ti, ^{44}Sc, ^{42}Ca, ^{41}K, ^{41}Ca, ^{39}K, ^{38}Ar and ^{37}Ar. Unfortunately, the 3α and 2α channels feeding ^{36}Ar and ^{40}Ca are only weakly populated. In the case of ^{40}Ca, it is known that the main gamma de-excitation flux of the deformed states is collected in the g.s. transition from the 2^+ state at 3905 keV [31]. For such a relatively large γ-ray energy, the efficiency of GASP is rather small and moreover this γ-ray region is strongly polluted by other γ rays from lighter nuclei produced via the reaction ^{24}Mg + ^{12}C (target backing). In the spectrum of ^{40}Ca, the lowest energy γ-ray is a $5^- \rightarrow 3^-$ transition, which has an energy of 754.7 keV. This γ-ray has been observed in the $\gamma-\gamma$ spectrum but unfortunately its intensity was weak. We have thus to conclude that the 2α ^{40}Ca channel was only weakly excited at the resonant bombarding energy. This energy is probably too high for the 2α channel, because the strongest channels fed at the resonance energy are those with $\geqslant 3$ particles emitted in the exit channel.

The ON/OFF resonance ratio (R) for the eight nuclei fed by fusion–evaporation is lower than the one obtained for the inelastic channels ($R \sim 2$), but in view of the care taken to extract this ratio, we think that the effect is real. As seen in Table 2, the ratio varies from 0.83 to 1.07, R is lower than 1 for ^{44}Sc, ^{41}K, ^{41}Ca, ^{38}Ar and ^{37}Ar, channels which present a 'lack' of flux, whereas a resonant effect is observed for ^{45}Ti, ^{42}Ca and ^{39}K for which $R \geqslant 1$. The maximum difference in R observed is around 25% and we thus believe that a resonant effect is effectively there. We would like to propose a possible scenario, which is based on reaction dynamics considerations. In the ^{24}Mg + ^{24}Mg reaction, before complete fusion into a ^{48}Cr nucleus, light particles could be emitted from the very deformed composite system. From such a pre-equilibrium state, the flux evacuated could feed the residues with $R \geqslant 1$. On a longer time scale, complete fusion into ^{48}Cr occurs and the subsequent evaporated particles are feeding the residues with $R < 1$. It is thus tentatively proposed that part of the resonant flux is carried away by this pre-equilibrium emitted particles and there is thus a lack of flux in the other residues. Of course, this hypothesis could be checked by measuring the angular and energy distributions of these light particles in coincidence with the residues of interest, a similar effect has been seen in the decay of the neighbouring ^{46}Ti in similar spin and excitation energy conditions [34].

As shown in Fig. 14, a resonant effect has been seen after evaporation of three particles from the composite ^{48}Cr nucleus, which creates the nuclei ^{45}Ti ($2pn$), ^{42}Ca ($\alpha 2p$) and ^{39}K ($2\alpha p$) whose ratios R are respectively 1.07, 1.03 and 1. If the number of emitted particles is larger, the ratio R is decreasing and becomes smaller than 1.

A possible explanation of this observation is that the high spin resonant flux feeds the residues ^{45}Ti, ^{42}Ca and ^{39}K via a fusion pre-equilibrium process which allows to evaporate particles from
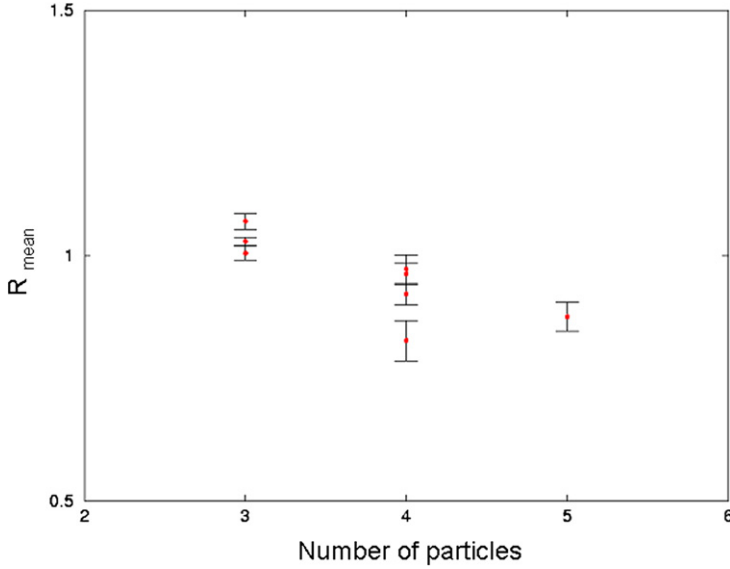
Fig. 14. Average of the ON/OFF resonance ratio for the fusion–evaporation channels as a function of the number of emitted particles.

the deformed composite system. The other residues are fed in a more statistical way from the lower compound nucleus angular momenta after complete fusion of two ^{24}Mg. In other words, there is a possible time selection (dynamical effect) in the de-excitation process of the resonance through certain fusion channels.

An important resonant effect has been observed in the inelastic channels involving the 2_1^+ and 4_1^+ states of ^{24}Mg. A weaker effect has been seen in certain fusion–evaporation channels. A link between the deformation in the entrance and in the exit channel could not be established due to the weak population, at the resonance bombarding energy, of ^{40}Ca, where superdeformation is known to exist [31,32].

4. Conclusion

The present work deals with the ^{24}Mg + ^{24}Mg system and especially with the $J^\pi = 36^+$ resonance situated at $E_{CM} = 45.7$ MeV. Two experiments were performed at the Tandem accelerator in Legnaro to look at ON and OFF resonance effects in the inelastic and fusion–evaporation de-excitation channels. Our main goal was to establish the connection of the resonance with molecular states of the deformed ^{48}Cr composite system.

Concerning the inelastic channels, the results have been obtained using the PRISMA spectrometer in coincidence with the γ CLARA array. For an excitation energy between 0 and 10 MeV, the resonant flux is essentially carried away by channels involving the ^{24}Mg 0_1^+, 2_1^+ and 4_1^+ g.s. members. This result is in a good agreement with the molecular model proposed by Abe and Uegaki and strengthens the argument in favor of the formation of a ^{48}Cr nuclear molecule.

It is known that for the ^{24}Mg + ^{24}Mg reaction, the elastic and inelastic channels are ten times stronger than the α transfer channels and that all the direct reaction channels absorb only 30%

of the resonance flux [6,9]. This is the reason why a second experiment has been performed with the GASP γ array coupled with the EUCLIDES Si detector on the fusion–evaporation channels. Weak resonant effects have been discovered for some of these channels such as ^{45}Ti, ^{42}Ca and ^{39}K. In addition, the yrast states of the different residues are selectively populated by the fusion–evaporation process, but no clear proof of the selective feeding of deformed states in the residues by a deformed composite system has been found.

A fast rotating ^{48}Cr undergoes a Jacobi shape transition which implies a very prolate shape for the nucleus just before the fission. We propose that this exotic ^{48}Cr shape is populated by the $J^{\pi} = 36^{+}$ resonance of the ^{24}Mg $+$ ^{24}Mg reaction and corresponds to a ^{24}Mg $-$ ^{24}Mg molecular state.

In conclusion, from the results obtained in the two experiments, it is obvious that there is still some resonant flux missing. It is possible that such flux could be found in the decay of the resonance through the giant dipole resonance as proposed in the case of the neighbouring fast rotating ^{46}Ti nucleus [34,35] and also through eventual interband E2 transitions between resonant molecular states which in the case of the studied $J^{\pi} = 36^{+}$ resonance are predicted to be particularly enhanced [8].

Acknowledgements

References

[1] F. Haas, Y. Abe, Phys. Rev. Lett. 46 (1981) 1667.
[2] C. Beck, Y. Abe, N. Aissaoui, B. Djerroud, F. Haas, Phys. Rev. C 49 (1994) 2618.
[3] C. Beck, Y. Abe, N. Aissaoui, B. Djerroud, F. Haas, Nucl. Phys. A 583 (1995) 269.
[4] R.W. Zurmühle, P.H. Kutt, R.R. Betts, S. Saini, F. Haas, O. Hansen, Phys. Lett. B 129 (1983) 384.
[5] A.H. Wuosmaa, R.W. Zurmühle, P.H. Kutt, S.F. Pate, S. Saini, M.L. Halbert, D.C. Henley, Phys. Rev. C 41 (1990) 2666.
[6] S. Saini, R.R. Betts, R.W. Zurmühle, P.H. Kutt, D.K. Dichter, Phys. Lett. B 185 (1987) 316.
[7] E. Uegaki, Y. Abe, Phys. Lett. B 231 (1989) 28.
[8] E. Uegaki, Prog. Theor. Phys. Suppl. 132 (1998) 135.
[9] R.W. Zurmühle, in: M. Brenner, T. Lönnroth, F.B. Malik (Eds.), Clustering Phenomena in Atoms and Nuclei, Springer-Verlag, Berlin, 1992, p. 380.
[10] A.M. Stefanini, et al., Nucl. Phys. A 701 (2002) 217.
[11] A. Gadea, et al., Eur. Phys. J. A 20 (2004) 193.
[12] D. Bazzacco, et al., in: Proceedings of the International Conference on Nuclear Structure at High Angular Momentum, vol. II, Ottawa, 1992, p. 376.
[13] http://gasp.lnl.infn.it.
[14] E. Farnea, et al., LNL Annual Report, 2005, p. 173.
[15] S. Szilner, et al., Phys. Rev. C 76 (2007) 024604.
[16] G. Montagnoli, et al., Nucl. Instrum. Methods Phys. Res. A 547 (2005) 455.
[17] S. Beghini, et al., Nucl. Instrum. Methods Phys. Res. A 551 (2005) 364.
[18] D.G. Jenkins, et al., Phys. Rev. C 71 (2005) 041301.
[19] C.M. Jachcinski, D.G. Kovar, R.R. Betts, C.N. Davids, D.F. Geesaman, C. Olmer, M. Paul, S.J. Sanders, J.L. Yntema, Phys. Rev. C 24 (1981) 2070.
[20] F.W. Prosser, S.V. Reinert, D.G. Kovar, G. Rosner, G.S.F. Stephans, J.J. Kolata, C.F. Maguire, A. Szanto de Toledo, E. Szanto, Phys. Rev. C 40 (1989) 2600.
[21] N. Rowley, private communication.
[22] A.J. Sierk, Phys. Rev. C 33 (1986) 2038.
[23] K.A. Farrar, et al., Phys. Rev. C 54 (1996) 1249.

[24] A.T. Hasan, et al., Phys. Rev. C 49 (1994) 1031.
[25] A. Maj, M. Kmiecik, N. Schunck, J. Styczen, AIP Conf. Proc. 802 (2005) 264.
[26] K. Pomorski, J. Dudek, Phys. Rev. C 67 (2003) 044316.
[27] J. Dudek, et al., Eur. Phys. J. A 20 (2004) 15.
[28] J. Dudek, private communication.
[29] S. Thummerer, et al., J. Phys. G 27 (2001) 1405.
[30] C.E. Svensson, et al., Phys. Rev. Lett. 85 (2000) 2693.
[31] E. Ideguchi, et al., Phys. Rev. Lett. 87 (2001) 222501.
[32] C.J. Chiara, et al., Phys. Rev. C 67 (2003) 041303.
[33] M. Lach, et al., Eur. Phys. J. A 16 (2003) 309.
[34] M. Kmiecik, et al., Acta Phys. Pol. B 38 (2007) 1437.
[35] A. Maj, et al., Nucl. Phys. A 731 (2004) 319.